Graphite-Epoxy Electrodes Modified with Functionalised Carbon Nanotubes and Chitosan for the Rapid Electrochemical Determination of Dipyrone

Rasa Pauliukaite[1], Mariana Emilia Ghica[1], Orlando Fatibello-Filho[1,2] and Christopher M.A. Brett[*,1]

[1]*Departamento de Química, Faculdade de Ciências e Tecnologia, Universidade de Coimbra, 3004-535 Coimbra, Portugal*

[2]*Departamento de Química, Universidade Federal de São Carlos, C.P. 676, 13560-970 São Carlos-SP, Brazil*

Abstract: A rapid electrochemical procedure for the determination of dipyrone was successfully developed at a carbon nanotube modified graphite-epoxy resin composite (GrEC) electrode. The composite electrode was used as support on which multi-walled carbon nanotubes (MWCNT) were immobilised by 1-ethyl-3-(3-dimethylaminopropyl) carbodiimide together with N-hydroxysuccinimide (EDC-NHS) in a chitosan (Chit) matrix. The electrochemical behaviour of dipyrone at this electrode in different buffer electrolytes with pH values between 5.0 and 8.0 was explored using cyclic voltammetry, differential pulse voltammetry, and electrochemical impedance spectroscopy, and comparison with a conventional glassy carbon electrode was made. Dipyrone was best determined by differential pulse voltammetry with a low limit of detection of 1.4 μM. Application to commercial samples was demonstrated.

Keywords: Dipyrone, functionalised carbon nanotubes, cyclic voltammetry, differential pulse voltammetry, electrochemical impedance spectroscopy.

1. INTRODUCTION

Dipyrone, known as sodium metamizole or sodium [(2,3-dihydro- 1,5-dimethyl- 3-oxo- 2-phenyl- 1*H*- pyrazol- 4-yl) methylamino] methanesulfonate (chemical structure in Fig. **1A**), is an analgesic prodrug with an antipyretic effect commonly used as a powerful painkiller. It was introduced into clinical practice in 1922 and is still currently used in many countries [1]; however, it was withdrawn from the drug market in the UK and US in the 1940s due to side effects, one of them being agranulocytosis [2]. Despite this, there has been a number of studies since then related to dipyrone metabolism [3] and degradation [4], its interaction with other compounds [5] and its influence on human health, e.g., respiratory function [6], and pathogenic risks to embryos [2, 7].

Methods reported in the recent literature for monitoring and quantifying dipyrone are usually liquid chromatography, including HPLC [8-10], chemiluminescence in the presence of MnO_2 [11], and flow injection analysis with various detection techniques [12-16]. Electrochemical determination has been reported using differential pulse voltammetry (DPV) [17], square wave voltammetry (SWV) [18], and cyclic voltammetry (CV) [18-20].

Carbon nanotubes (CNTs) are attractive materials for a wide range of applications, owing to their unique structure, mechanical strength and electronic properties [21-32]. CNTs are able to decrease the overpotential and increase the rate of reaction of various electroactive species; thus they are more and more often applied in electroanalytical chemistry as electrode modifiers [22, 23]. Such modified electrodes generally show better electrochemical performance than conventional carbon electrodes [22, 29]. As has been demonstrated, the electroactivity of CNTs is due to the presence of reactive groups on their surface and surface defects of the nanotubes [25-27]. CNT-modified electrodes represent different designs of electrochemical sensors and biosensors [21-25].

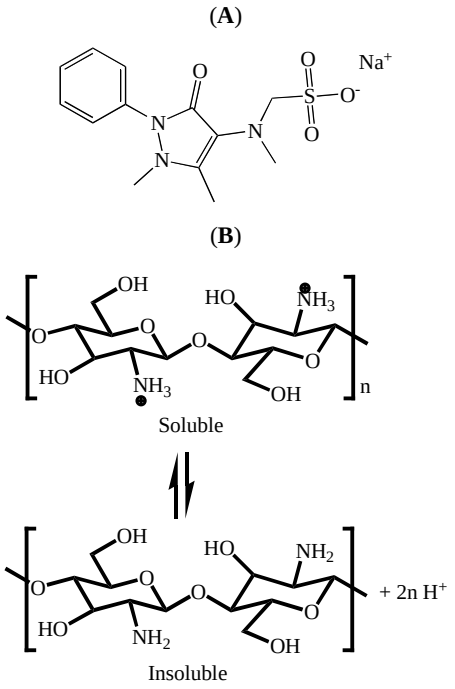

Fig. (1). Chemical structure of (**A**) dipyrone (sodium [(2,3-dihydro-1,5-dimethyl-3-oxo-2-phenyl-1*H*-pyrazol-4-yl) methylamino] methane-sulfonate); (**B**) equilibrium of chitosan in solution.

*Address correspondence to this author at the Departamento de Química, Faculdade de Ciências e Tecnologia, Universidade de Coimbra, 3004-535 Coimbra, Portugal; Tel/Fax: +351239835295; E-mail: brett@ci.uc.pt

1386-2073/10 $55.00+.00

The major drawback of using CNTs as electrode modifiers is their insolubility in all solvents. Several strategies have been proposed to disperse them, such as end and sidewall functionalisation [5, 33, 34], use of surfactants with sonication [35], polymer wrapping [36], and covalent binding [21].

Chitosan is a linear β-1,4-linked polysaccharide that is obtained by the partial deacetylation of chitin, a major component of the shells of crustaceans such as crab, shrimp, and crawfish. Since chitin deacetylation is incomplete, chitosan is formally a copolymer composed of glucosamine and N-acetylglucosamine. The chemical and biological properties of chitosan are determined by reactive amino and hydroxyl groups in its linear polyglucosamine high molar mass chains which are amenable to chemical modification [37-41]. Moreover, amino groups transform chitosan into a cationic polyelectrolyte ($pK_a \cong 6.5$), one of the few found in nature. Its basicity ensures chitosan's unique properties: it is soluble in aqueous acidic media at pH lower than 6.5 and, when dissolved, possesses a high positive charge due to the $-NH_3^+$ groups (Fig. **1B**); therefore, it can easily adhere to negatively-charged surfaces and aggregate with polyanionic compounds as well as chelating with various metal cations. Besides its good adhesion, chitosan has a high permeability toward both water and a number of anions and cations, a high mechanical strength, an excellent film-forming ability, and, finally, it is a very good matrix for enzyme and/or biomacromolecule immobilisation [18].

Methods for chitosan film preparation described in the literature [23] can be broadly divided into four groups: solvent evaporation, neutralisation, crosslinking and ionotropic gelation methods.

The present work focuses on the determination of dipyrone using a graphite-epoxy resin composite (GrEC) electrode modified with functionalised multi-wall carbon nanotubes (MWCNT) immobilised into a chitosan matrix by means of 1-ethyl-3-(3-dimethylaminopropyl) carbodiimide together with N-hydroxysuccinimide (EDC-NHS). Cyclic voltammetry, differential pulse voltammetry and electrochemical impedance spectroscopy were used in different pH buffer electrolytes in order to elucidate the dipyrone electrochemical process. Comparison was made with the electrochemical behaviour at an unmodified glassy carbon electrode. Application to fast analysis of commercial samples was demonstrated.

2. EXPERIMENTAL

2.1. Apparatus

Cyclic voltammetry and differential pulse voltammetry were performed using a μAutolab potentiostat (Metrohm-Autolab, Netherlands) running with GPES 4.9 software. Electrochemical impedance measurements were carried out using a Solartron 1250 Frequency Response Analyser, coupled to a Solartron 1286 Electrochemical Interface (Ametek, UK) controlled by ZPlot software. The frequency range used was 65 kHz to 0.1 Hz with 10 frequencies per decade, and integration time 60s. The pH measurements were done with a CRISON 2001 micro pH-meter (Crison, Spain). All experiments were performed at room temperature, 25 ± 1°C.

2.2. Chemicals

Multi-walled carbon nanotubes (MWCNTs) were obtained from NanoLab (USA). Araldit epoxy resin and Araldit hardener were purchased from Ceys S.A. (Spain). Graphite powder (grade #38) was obtained from Fisher Scientific Corporation (USA). Chitosan (Chit) of low molecular weight with a degree of deacetylation of 80 % were obtained from Aldrich (Germany), 1-ethyl-3-(3-dimethylaminopropyl) carbodiimide (EDC) were purchased from Sigma (Germany) and N-hydroxysuccinimide (NHS) was from Fluka (Germany). Dipyrone was obtained from Fluka. Millipore Milli-Q nanopure water (resistivity > 18 MΩ cm) was used for the preparation of all solutions.

2.3. Pre-Treatment of Multi-Walled Carbon Nanotubes

Multi-walled carbon nanotubes (MWCNT) were purified and functionalised as described elsewhere [28]. A mass of 120 mg of MWCNT was stirred in 10 mL of a 3 M nitric acid solution for 20 h. The solid product was collected on a filter paper and washed several times with nanopure water until the filtrate solution became neutral (pH ≅ 7). The functionalised MWCNTs obtained were then dried in an oven at 80 °C for 24 h. Nitric acid usually causes significant destruction of carbon nanotubes and introduces –COOH groups at the ends or at the sidewall defects of the nanotube structure.

2.4. Preparation of Graphite-Epoxy Composite Electrode

Graphite-epoxy composite electrodes were used as electrode substrates. These were prepared using graphite powder and Araldit epoxy resin/hardener by hand-mixing in the ratio 70:30 (m/m), as described previously [42]. The resulting paste was placed into the tip of a 1 mL insulin plastic syringe, and a copper rod with diameter equal to the inner size of the syringe was inserted to give external electrical contact. Before each use, the surface of the composite electrode was wetted with Milli Q water and then thoroughly smoothed, first with abrasive paper and then with polishing paper (Kemet, UK).

2.5. Preparation of the Film Electrodes Containing Functionalised MWCNTs

A 1.0 % m/m chitosan (Chit) stock solution was prepared by dissolving 100 mg of Chit powder in 10 mL of 1.0 % v/v acetic acid solution and stirred for 3 h at room temperature until complete dissolution occurred. The Chit solution was stored at 4°C when not in use.

A dispersion of 1.0 % m/v functionalised MWCNTs in 1.0 % m/m chitosan was prepared by sonication of 2 mg of functionalised MWCNTs in 200 μL of 1.0 % m/m Chit in 1.0 % v/v acetic acid solution for 2 h.

The film electrode, obtained using the 1.0 % m/v functionalised MWCNTs in 1.0 % m/m chitosan, was prepared following the procedure:

1) dropping 10 μL of 1 % m/v MWCNTs in 1.0 % m/m Chit on the GrEC and leaving to dry. After solvent evaporation, another aliquot of 10 μL of MWCNT dispersion was added and the electrode was again left

for solvent evaporation at room temperature in air for approximately 1 h;

2) 10 μL of 0.1 M phosphate buffer saline (pH 7.0) solution was dropped on the surface and left to dry for 40 min and this step was then repeated, in order to deprotonate the amino groups of Chit by changing the pH at the electrode surface;

3) finally, 10 μL of 0.5 % m/v EDC-0.5 % m/v NHS in the same buffer solution was dropped on the surface and left to dry for 2 h.

2.6. Preparation and Detection of Dipyrone in Pharmaceutical Samples

Samples were prepared by dissolving commercially available drugs: Metamizol (generic) and Nolotil, which both contain 575 mg of magnesium metamizol per capsule (according to the label), in 0.1 M phosphate buffer pH 7.0. Prior to measurement, a calibration curve with dipyrone standard solution was made by differential pulse voltammetry. For sample determination, a voltammogram was first recorded in buffer solution, then an aliquot of aqueous drug solution was added and analysed, the result being compared with the calibration data of dipyrone in buffer. Each sample was analysed six times.

3. RESULTS AND DISCUSSION

3.1. Electrochemical Behaviour of Dipyrone

In previous studies, it was found that graphite-epoxy composite electrodes modified with CNTs cross-linked to chitosan with EDC-NHS cross-linker showed the best electrochemical behaviour compared to other cross-linkers studied [43, 44]. This modified electrode was therefore chosen for the study and determination of dipyrone. The electrode was first characterised electrochemically in the presence of the drug using cyclic voltammetry and electrochemical impedance spectroscopy and determination of dipyrone was then performed by differential pulse voltammetry.

3.1.1. Voltammetric Characterisation

Dipyrone is a complex compound and its electrochemical behaviour is also complicated. In order to shed light on the dependence of the electrochemical oxidation of dipyrone on the electrode material, CVs and DPVs were recorded at graphite-epoxy composite electrodes modified with MWCNT in chitosan matrix and at glassy carbon electrodes in phosphate buffer solution, pH 7.0.

Fig. (**2**) presents CVs obtained with different dipyrone concentrations at a glassy carbon electrode (GCE) (Fig. **2A**), and at a graphite-epoxy composite electrode modified with multi-walled nanotubes in a chitosan matrix (GrEC/MWCNT-Chit) (Fig. **2B**), in order to examine the influence of the electrode material. Three irreversible-shaped peaks were observed at the GCE (Fig. **2A**) at +0.30, +0.57, and + 0.75 V *vs* SCE. The current peaks increase in height with higher dipyrone concentrations. Similar peaks have been observed in [19] at carbon paste electrodes and all peaks are attributed to a gradual oxidation of dipyrone [18, 19]. CVs recorded under the same conditions at GrEC/MWCNT-Chit electrodes, also exhibited three irreversible oxidation peaks, but slightly shifted compared to GCE: +0.12 (peak I), +0.51 V (peak II) and +0.79 V (peak III) *vs* SCE. The peaks at +0.12 and +0.51 V appear as double peaks and with an increase in dipyrone concentration the separation between these peaks also increases.

(**A**)

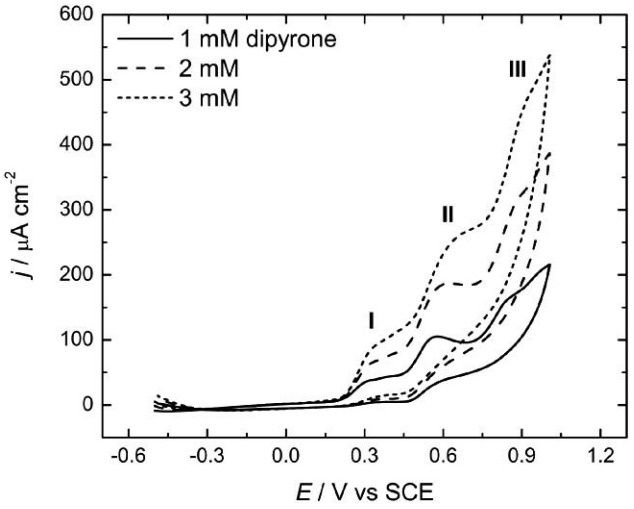

(**B**)

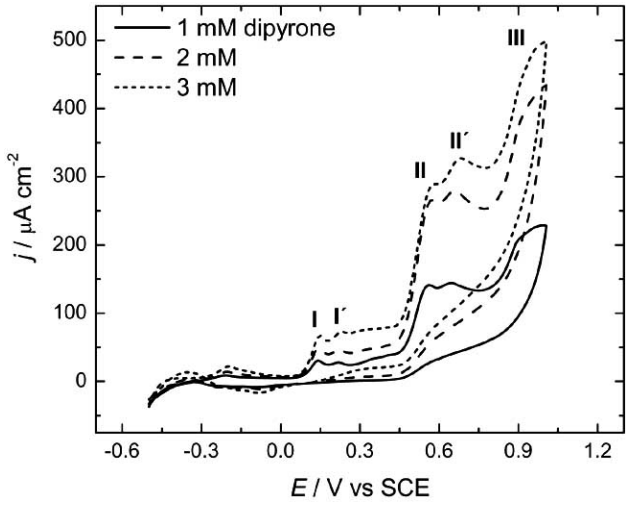

Fig. (2). CVs of different concentrations of dipyrone at GCE (**A**) and GrEC/MWCNT-Chit (**B**) in 0.1 M PBS, pH 7.0. Potential scan rate 25 mV s^{-1}.

Using differential pulse voltammetry, three oxidation peaks were also observed at both electrodes by DPV but shifted (especially at GCE) to less positive potentials: at ca. +0.2 (I), +0.55 (II) and +0.7 V (III) at GCE, and at +0.1 (I), +0.47 (II) and +0.9 V (III) *vs* SCE at the MWCNT-Chit modified electrode, as seen from Fig. (**3**). Thus, the first two oxidation peaks occur at lower potential values at GrEC/MWCNT-Chit than at GCE, demonstrating the electrocatalytic effect of the modified electrode with respect to GCE.

In order to clarify the mechanism of dipyrone oxidative degradation, CVs were recorded (i) at different scan rates at pH 7.0 and (ii) at different pH at scan rate 25 mV s^{-1}. DPVs

for this purpose were recorded only at different pH values at constant scan rate.

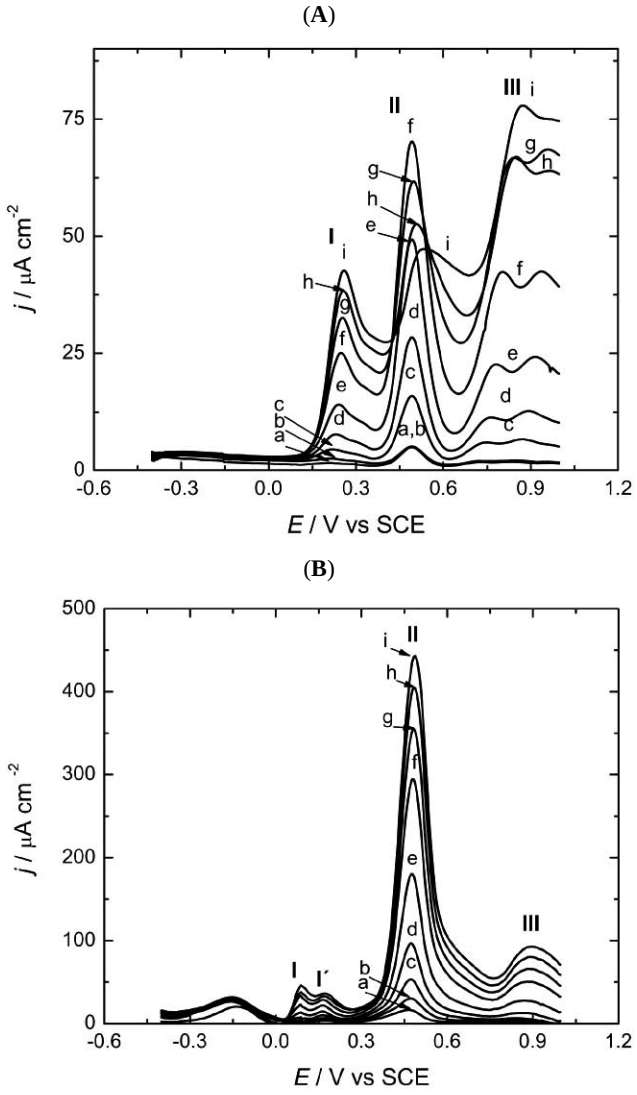

Fig. (3). DPVs recorded at GCE (**A**) and GrEC/MWCNT-Chit (**B**) film electrode in 0.1 M phosphate buffer, pH 7.0, at 10 mV s^{-1} with dipyrone concentrations (mM): a) 0.05, b) 0.1, c) 0.2, d) 0.4, e) 0.8, f) 1.5, g) 2.0, h) 2.5 and i) 3.0.

Cyclic voltammograms recorded at different scan rates in PBS, pH 7.0 in the presence of 2 mM of dipyrone are shown in Fig. (**4**). It was found that with an increase in scan rate the separation of the double peaks also increased and an additional peak appeared at +0.41 V (peak IV). All peaks were analysed by plotting the peak current versus scan rate (not shown) and versus square root of scan rate; all showed a linear dependence on the square root of the scan rate up until 30 mV s^{-1} (Table **1**), showing that processes are controlled by diffusion of the analyte at lower scan rates and by chemical reaction at higher scan rates since the peak height becomes independent of scan rate. The last peak, III, was not well defined and was therefore difficult to analyse.

Cyclic (Fig. **5**) and differential pulse voltammograms recorded in different pH buffer electrolytes between 5.0 and 8.0 exhibited different behaviour. At lower pH values (5.0

Table 1. Peak Current Dependence on the Square Root of the Scan Rate, Data from CVs in Fig. (4)

Peak	I *vs* $v^{1/2}$/ μA $mV^{-1/2}$ $s^{1/2}$
I	3.59±0.31
I′	3.40±0.20
II	4.54±0.09
II′	4.86±0.16
IV	4.61±0.20

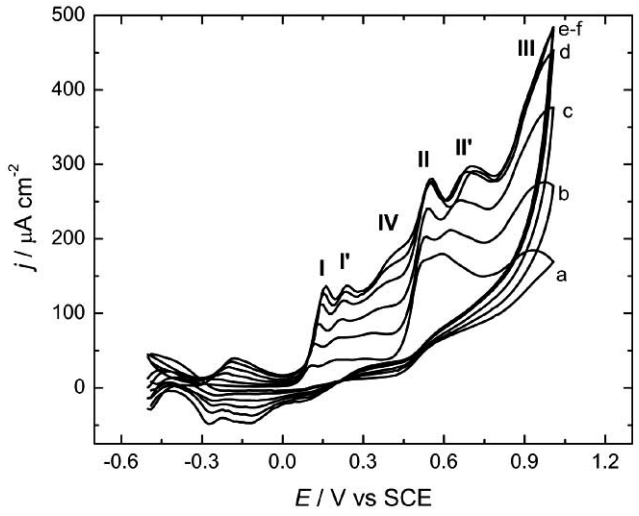

Fig. (4). CVs at GrEC/MWCNT-Chit electrode in 0.1 M PBS pH 7.0 and 2 mM dipyrone. Potential scan rate mV s^{-1}: a – 5; b – 10, c – 20, d – 30; e – 40; f – 50.

and 6.0) three irreversible oxidation peaks appeared, the first is a double peak. At higher pH values, dipyrone oxidation occurs as is reported above at pH 7.0: three irreversible oxidation peaks with double 1st and 2nd peaks. The first double peak is less visible at pH 5.0, even at higher dipyrone concentrations. Beginning at pH 6.0, the 2nd peak is better observed mainly at higher concentration and an additional peak also appears between the 1st and 2nd peaks (peak IV), and, at pH 8.0 the additional peak is perfectly clear. This peak might be attributed to the oxidation of an adsorption product, which is more visible at higher pH. DPVs recorded in the same buffer solutions for 2 successive scans showed, in all cases, a decrease in the signal in the second voltammogram, probably due to blocking adsorption of dipyrone or its oxidation products at the electrode surface. Considering peak II, which is more pronounced, and monitoring the adsorption at different pH values, it was observed that at pH 8.0 dipyrone adsorbs more (31 %) followed by pH 6.0 and 7.0 (27 %) and at pH 5.0 adsorption was the weakest (9 %). However adsorption is stronger at lower drug concentrations.

The peak width at half height of peak II was around 100 mV in all buffers studied, consistent with a one-electron transfer process. For 1 mM dipyrone, the highest current was obtained at pH 8.0 for peaks I´ and II, and for I at pH 7.0, by

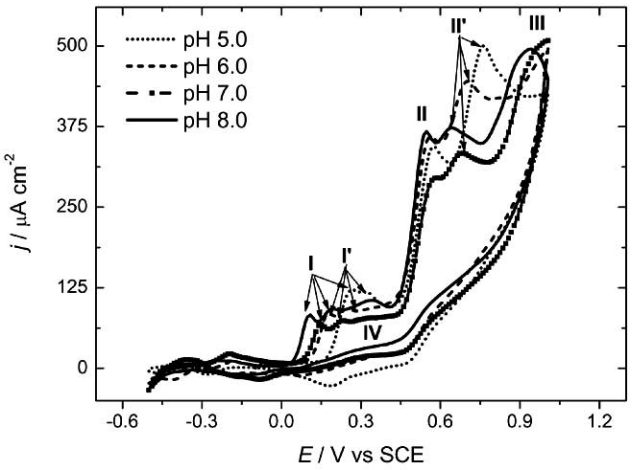

Fig. (5). CVs of 3 mM dipyrone at GrEC/MWCNT-Chit electrode in 0.1 M PBS at different pH values. Potential scan rate 25 mV s^{-1}.

both CV and DPV. At higher concentrations of dipyrone (2 and 3 mM) this is reversed: the highest response for peaks I´ and II was exhibited in pH 7.0 solution and for peak I in pH 8.0 solution (not shown).

The peak potential for the first double peak moved linearly to less positive values with increasing pH, with slopes 39.4 mV dec^{-1} for peak I and 34.2 mV dec^{-1} for peak I´, showing that two electrons per proton are involved in the electrochemical reaction, as in [45]. Peak II almost maintained its position in CV as well as in DPV, so that no protons are involved.

A similar behaviour was observed in [19] where a carbon paste electrode modified with *N,N'*-ethylene*bis*(salicylide-neiminato)oxovanadium(IV) complex ([VO(Salen)]) was used. In this study, the authors monitored the dependence of peak potential with pH of the peak occurring around 0.6 V, which is the nearest to the potential of peak II in this study. In [19] and here, the peak potentials moved to more positive values with increase in dipyrone concentration, showing that the drug is more stable at higher concentration, therefore more difficult to oxidise. The highest response was not exhibited at the same pH for all the peaks. However, for 1 mM dipyrone, peak I (CV) has a maximum in pH 7.0 solution and peak II continuously increases in height up to pH 8.0.

The peak at -0.2 V (Figs. **2B**, **4**, **5**), appears probably due to reaction of the dipyrone $-SO_3^-$ group with $-NH_2$ groups of chitosan and is controlled by dipyrone adsorption on the electrode surface.

The double peaks (I´ and II´) and additional peak IV (Fig. **4**) appear due to reaction of the dipyrone oxidation products either with chitosan or with the functional groups of carbon nanotubes or the mechanism of electrochemical reactions changes, i.e. maybe the oxidation products adsorb more easily at GrEC/MWCNT-Chit than at GCE. These peaks increase linearly in height with increase in dipyrone concentration but the linear response range at GrEC/MWCNT-Chit was shorter than at GCE. The easiest oxidation step is loss of the sulphite group and the next step is oxidation of methyl group at the outer nitrogen to methyl amino group and then to methyl-methanal amino or to simple amine (Fig. **6**); such metabolites of dipyrone can be found during its oxidation [4, 46].

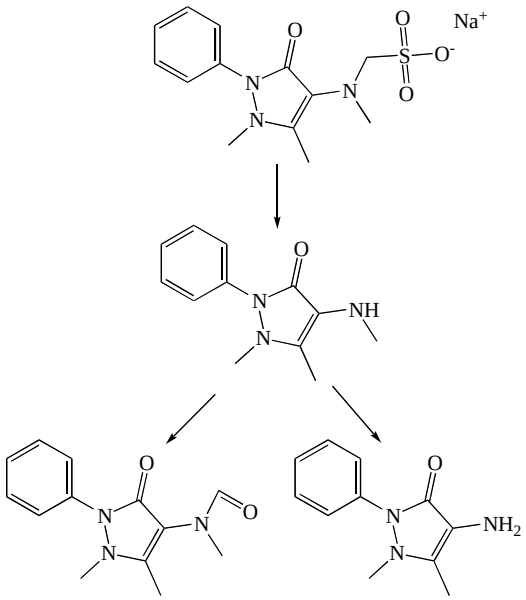

Fig. (6). Scheme of possible dipyrone degradation.

Cyclic and differential pulse voltammetry demonstrate that the electrooxidation of dipyrone at GrEC/MWCNT-Chit is easier than at glassy carbon electrodes, the oxidation mechanism being the same.

3.1.2. Electrochemical Impedance Spectroscopy

Electrochemical impedance spectra were recorded in phosphate buffer solution in the absence and presence of dipyrone at GCE and GrEC/MWCNT-Chit electrodes. Applied potentials were 0.0, +0.32, +0.45, +0.60, and OCP (~+0.15 V) at GCE and 0.0, +0.15, +0.47, +0.57, +0.66 V *vs* SCE (where oxidation peaks of dipyrone were found) and at OCP (~+0.02 V) at GrEC/MWCNT-Chit, where no peaks were observed. The spectra obtained at the GCE had higher impedance values than those at the carbon nanotube modified composite electrode; this confirms better conductivity of the modified electrode. No changes were observed in the impedance after dipyrone addition either at 0.0 V or at OCP at the GrEC/MWCNT-Chit electrode, but there were very slight changes at GCE at OCP (not shown). At all other potentials, visible changes were obtained after each dipyrone addition in the middle and low frequency region, more obvious at the GCE. Fig. (**7**) presents complex plane impedance spectra at + 0.45 V and +0.47 V *vs* SCE in 0.1 M phosphate buffer solution, pH 7.0, with addition of 0, 1, and 2 mM dipyrone at GCE and GrEC/MWCNT-Chit electrodes respectively. A decrease of impedance values after dipyrone addition was observed at the GCE unlike at the GrEC/MWCNT-Chit electrode. Similar spectra were obtained at other potentials as reported previously [47].

The spectra at the GCE at all potentials with and without dipyrone addition were analysed by fitting to an equivalent electrical circuit, consisting of the cell resistance, R_Ω, coupled with two complex elements in series consisting of 1) the charge transfer resistance, R_{ct}, in parallel with a constant

(**A**)

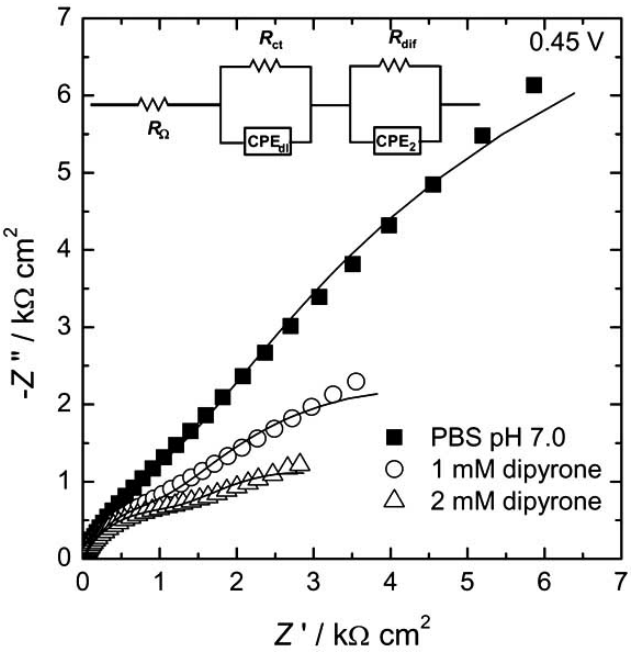

(**B**)

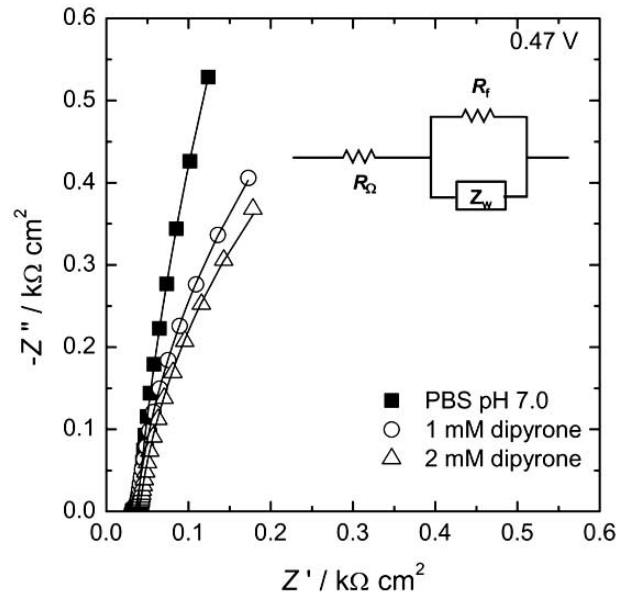

Fig. (7). Complex plane impedance spectra at 0.45V at GCE (**A**) and at 0.47 V *vs* SCE at GrEC/MWCNT-Chit (**B**) electrode in 0.1 M NaPBS pH 7.0, in the presence and absence of dipyrone. Lines indicate equivalent circuit fitting.

phase element, CPE_{dl}, as non-ideal double layer capacitance and 2) a diffusion resistance, R_{dif}, in parallel with a constant phase element, CPE_2, as a non-ideal capacitance (Fig. **7A**, inset). The data obtained from equivalent circuit fitting are presented in Table **2**. R_Ω was ~11 Ω cm^2, independent of potential or dipyrone addition. At all potentials C_{dl} decreased with increase in dipyrone concentration, but R_{dif} decreased in most cases after the first dipyrone addition and increased after the second aliquot, demonstrating more difficult charge transfer at higher analyte concentrations (as observed by cyclic voltammetry, section 3.1.1), probably due to adsorption on the electrode surface. Both the diffusion resistance, R_{dif}, and C_2 values decreased with increase of analyte concentration, as expected.

Spectra at the GrEC/MWCNT-Chit electrode were different and other equivalent electrical circuits were needed, see also [47]. At OCP, 0.0, and +0.15 V *vs* SCE (the last without dipyrone addition), where no redox process has occurred, fitting could be done just with R_Ω in series with an infinite open Warburg element, W_o. However, the spectra at all the other potentials tested were not linear in the complex plane plots at low frequencies and, therefore, a film resistance, R_f, was introduced in parallel with W_o. R_Ω was 31 Ω cm^2 in buffer at all potentials and hardly changed with addition of 1 mM of dipyrone, but increased slightly to 34 Ω cm^2 after another aliquot of 1 mM of dipyrone was added (Fig. **7B**). As expected, the cell resistance did not depend on applied potential, but the Warburg element parameters changed with addition of dipyrone. Detailed analysis of the spectra at GrEC/MWCNT-Chit electrode is described in [47].

The results obtained show that dipyrone analyte decreases film resistance and diffusion of the charged species through the film.

3.2. Determination of Dipyrone by Differential Pulse Voltammetry

Differential pulse voltammetry is an excellent technique for the analysis of electrochemically active substances owing to its good sensitivity and resolving power. DPVs recorded at both GCE and GrEC/MWCNT-Chit in 0.1 M phosphate buffer pH 7.0 with successive additions of dipyrone (Fig. **3**) showed that the sensitivity (or analytical signal) and the dependence on dipyrone concentrations was very different at the two types of electrode; however, both showed higher sensitivity to dipyrone using peak II than with the other peaks. The peak height of peaks I and II at GCE and peak II at GrEC/MWCNT-Chit electrode was plotted *vs* dipyrone concentration (not shown). The linear ranges obtained from the plots were found to be up to 2.5 and 0.4 mM dipyrone for peaks I and II, respectively, at GCE, and up to 1.5 mM dipyrone at the GrEC/MWCNT-Chit electrode. The sensitivity was: 3.65±0.04 μA cm^{-2} mM^{-1} (peak I/GCE), 23.9±0.8 μA cm^{-2} mM^{-1} (peak II/GCE), and 194±7 μA cm^{-2} mM^{-1} (peak II/GrEC/MWCNT-Chit electrode), showing that the modified GrEC gives higher sensitivity to dipyrone by a factor of 8. The limit of detection, calculated from the calibration data applying the 3σ method (three times standard deviation of the calibration curve divided by the slope) also was the lowest at the GrEC/MWCNT-Chit electrode (1.4 μM) following by peaks I (9.7 μM) and II at GCE (10.4 μM).

The analytical data achieved by using the present modified electrode are significantly better than those obtained in [17] by DPV: sensitivity 0.27 nA μM^{-1}, linear range up to 65 μM, LOD 2.37 μM. Other electrochemical methods also gave less good analytical parameters, such as amperometry with flow injection analysis [48]: sensitivity 81.06 μA mM^{-1}, linear range up to 25 μM, LOD 2.07 μM; or linear sweep voltammetry [19]: linear range up to 28 μM,

Table 2. Equivalent Circuit Fitting Data from Impedance Spectra at Glassy Carbon Electrode (See Fig. (7A) in 0.1 M Phosphate Buffer, pH 7.0 with and without Dipyrone (dipy)). OCP was ~ +150 mV *vs* SCE

E/V *vs* SCE	Solution Composition	R_{ct}/kΩ cm^2	C_{dl}/ μF cm^{-2} s^{n-1}	α_1	R_{diff}/kΩ cm^2	C_2/μF cm^{-2} s^{n-1}	α_2
OCP	Buffer	0.87	110	0.75	10.9	182	0.73
	+ 1 mM dipy	1.15	105	0.75	11.4	190	0.73
	+ 2 mM dipy	1.25	97	0.74	14.2	207	0.73
0.00	Buffer	0.78	130	0.75	19.9	209	0.73
	+ 1 mM dipy	0.86	132	0.76	17.6	233	0.75
	+ 2 mM dipy	1.37	139	0.71	16.6	246	0.73
0.32	Buffer	1.01	101	0.78	21.9	161	0.76
	+ 1 mM dipy	0.91	61	0.80	3.55	350	0.74
	+ 2 mM dipy	1.09	63	0.75	1.86	555	0.71
0.45	Buffer	1.21	84	0.80	20.5	142	0.78
	+ 1 mM dipy	1.01	64	0.79	6.59	256	0.73
	+ 2 mM dipy	1.20	59	0.75	3.40	404	0.71
0.60	Buffer	1.34	72	0.82	21.9	126	0.79
	+ 1 mM dipy	1.17	57	0.79	6.17	236	0.73
	+ 2 mM dipy	1.39	58	0.74	4.11	328	0.71

Table 3. Determination of Dipyrone Found in Commercial Drugs (*n*=6) by Differential Pulse Voltammetry

Drug	Concentration of Dipyrone Added, μM	Concentration of Dipyrone Found, μM	Recovery, %
Metamizol	500	471 ± 20	94
	172	162 ± 7	94
Nolotil	500	490 ± 10	98
	172	162 ± 8	94

LOD 7.2 μM; or by the turbidimetric method using Ag^+ ions, where the LOD was 130 μM [12].

3.3. Determination of Dipyrone in Commercial Samples

The GrEC/MWCNT-Chit electrode was used for the determination of dipyrone in two commercially available drugs: Metamizol (generic) and Nolotil. According to the label, both contain 575 mg of magnesium metamizol per capsule. Determination was performed by adding a certain aliquot of aqueous drug solution in 0.1 M phosphate buffer pH 7.0 to the same buffer solution, then recording DPV and comparing the result with the calibration data of dipyrone in buffer, see Section 2.6. In both cases, recovery was satisfactory using different concentrations of drugs (Table **3**) calculated from 6 measurements. The appearance of a yellowish colour in the drug solution as well as a small decrease (up to ~1 %) of the dipyrone DPV signal after each repetition of the measurement, suggested that the drug solution prepared from the capsules decomposed faster (probably due to additives) than a stock solution of dipyrone at room temperature. This probably caused the slightly low recovery values, and clearly demonstrates the necessity for a rapid method for sample analysis as soon as the sample is prepared, as is the case with the method developed in this paper.

Thus, the data obtained by DPV determination lead to the conclusion that GrEC/MWCNT-Chit electrodes can be used for fast and simple determination of dipyrone in neutral media with a low micromolar detection limit.

4. CONCLUSIONS

A graphite epoxy composite electrode modified with functionalised carbon nanotubes immobilised into chitosan matrix using 1-ethyl-3-(3-dimethylaminopropyl) carbodi-imide together with N-hydroxysuccinimide (EDC-NHS) was successfully used for the determination of dipyrone. The electrochemical behaviour of this drug was investigated by cyclic voltammetry, differential pulse voltammetry, and impedance spectroscopy and the results compared with those at glassy carbon electrodes. It was shown that carbon nanotubes improve the determination of dipyrone by shifting the oxidation potentials to lower values and increasing current response. The highest response was at different values of pH according to the peak analysed, nearly all of which shift to less positive values with increase in pH. Determination of dipyrone using differential pulse

voltammetry was far more sensitive at the graphite carbon nanotube modified electrode compared with glassy carbon, with a limit of detection of 1.4 μM. These results, and application to commercial samples, showed that this method is simple, fast and reliable for the determination of dipyrone and suggests that this type of modified electrode can be successfully employed for the determination of other analytes of this kind.

ACKNOWLEDGEMENTS

Financial support from Fundação para a Ciência e a Tecnologia (FCT), PTDC/QUI/65255/2006 and PTDC/QUI/65732/2006, POCI 2010 (co-financed by the European Community Fund FEDER) and CEMUC® (Research Unit 285), Portugal, is gratefully acknowledged. O.F.F. thanks CAPES/4383-07-9, UFSCar and the University of Coimbra for a visiting professorship. R.P. and M.E.G. thank FCT for postdoctoral fellowships SFRH/BPD/27075/2006, and SFRH/BPD/36930/2007, respectively.

REFERENCES

[1] Ergün, H.; Frattarelli, D.A.C.; Aranda, J.V. Characterization of the role of physicochemical factors on the hydrolysis of dipyrone. *J. Pharm. Biomed. Anal*., **2004**, *35*, 479-487.

[2] Bánhidy, F.; Ács, N.; Puhó, E.; Czeizel, A.E. A population-based case-control teratologic study of oral dipyrone treatment during pregnancy. *Drug Safety*, **2007**, *30*, 59-70.

[3] Bocca, C.C.; Basso, E.A.; Mosquetta, R. Conformational study of the four main dipyrone metabolites through theoretical methods: Electrostatic potential maps and NBO calculations. *Theochem-J. Molec. Struct.*, **2007**, *815*, 75-81.

[4] Pérez-Estrada, L.A.; Malato, S.; Agüera, A.; Fernández-Alba, A.R. Degradation of dipyrone and its main intermediates by solar AOPs. Identification of intermediate products and toxicity assessment. *Catalysis Today*, **2007**, *129*, 207-214.

[5] Müssig, K.; Pfäfflin, A.; Häring, H.U.; Schleicher, E.D. Dipyrone (metamizole) metabolites interfere with HPLC analysis of plasma catecholamines but not with the determination of urinary catecholamines. *Clin. Chem.*, **2006**, *52*, 1829-1831.

[6] Gulmez, S.E.; Tulunay, F.C.; Beder, S.; Kayacan, O.; Karnak, D. Does dipyrone have any effect on respiratory function in COPD patiens? *Respir. Med.*, **2006**, *100*, 828-834.

[7] Dal Pizzol, T.D.S.; Schüler-Faccini, L.; Mengue, S.S.; Fischer, M.I. Dipyrone use during pregnancy and adverse perinatal events. *Arch. Gynecol. Obstet.*, **2009**, *279*, 293-297.

[8] Di Nezio, M.S.; Pistonesi, M.F.; Centurión, M.E.; Palomeque, M.E.; Lista, A.G.; Fernández Band, B.S. A home-made hybrid system for the simultaneous determination of ergotamine, dipyrone and caffeine in pharmaceutical preparations. *J. Braz. Chem. Soc.*, **2007**, *18*, 1439-1442.

[9] Senyuva, H.Z.; Aksahin, I.; Ozcan, S.; Kabasakal, B.V. Rapid, simple and accurate liquid chromatography-diode array detection validated method for the determination of dipyrone in solid and liquid dosage forms. *Anal. Chim. Acta*, **2005**, *547*, 73-77.

[10] Golubitskii, G.B.; Budko, E.V.; Ivanov, V.M. Quantitative analysis of pentalgin N tablets by gradient and isocratic high-performance liquid chromatography. *J. Anal. Chem.*, **2006**, *61*, 67-71.

[11] Zhao, L.; Li, B.; Zhang, Z.; Lin, J.M. Chemiluminescent flow-through sensor for automated dissolution testing of analgin tablets using manganese dioxide as oxidate. *Sens. Actuat. B*, **2004**, *97*, 266-271.

[12] Marcolino-Jr., L.H.; Bonifácio, V.G.; Fatibello-Filho, O.; Teixeira, M.F.S. Flow injection turbidimetric determination of dipyrone using a solid-phase reactor containing silver chloride immobilized in a polyester resin. *Quim. Nova*, **2005**, *28*, 783-787.

[13] Marcolino-Jr., L.H.; Sousa, R.A.; Fatibello-Filho, O.; Moraes, F.C.; Teixeira, M.F.S. Flow-injection spectrophotometric determination of dipyrone in pharmaceutical formulations using ammonium molybdate as chromogenic reagent. *Anal. Lett.*, **2005**, *38*, 2315-2326.

[14] Oliveira, S.C.B.; Coelho, E.C.S.; Selva, T.M.G.; Santos, F.P.; Araújo, M.C.U.; Abreu, F.C.; Nascimento, V.B. A coulometric flow cell for in-line generation of reagent, titrant or standard solutions. *Microchem. J.*, **2006**, *82*, 220-225.

[15] Weinert, P.L.; Fernandes, J.R.; Pezza, L.; Pezza, H.R. Flow-injection spectrophotometric determination of novalgin in pharmaceuticals using micellar medium. *Anal. Sci.*, **2007**, *23*, 1383-1389.

[16] Medeiros, E.P.; Castro, S.L.; Formiga, F.M.; Santosa, S.R.B.; Araujo, M.C.U.; Nascimento, V.B. A flow injection method for biamperometric determination of dipyrone in pharmaceuticals. *Microchem. J.*, **2004**, *78*, 91-96.

[17] Baranowska, I.; Markowski, P.; Gerle, A.; Baranowski, J. Determination of selected drugs in human urine by differential pulse voltammetry technique. *Bioelectrochemistry*, **2008**, *73*, 5-10.

[18] Muralidharan, B.; Gopu, G.; Vedhi, C.; Manisankar, P. Voltammetric determination of analgesics using a montmorillonite modified electrodes. *Appl. Clay Sci.*, **2008**, *42*, 206-213.

[19] Teixeira, M.F.S.; Marcolino-Júnior, L.H.; Fatibello-Filho, O.; Dockal, E.R.; Cavalheiro, E.T.G. Voltammetric determination of dipyrone using a N,N´-ethylenebis(salicylideneaminato)oxovanadium(IV) modified carbon-paste electrode. *J. Braz. Chem. Soc.*, **2004**, *15*, 803-808.

[20] Basáez, L.A.; Peric, I.M.; Jara, P.A.; Soto, C.A.; Contreras, D.R.; Aguirre, C.; Vanýsek, P. Electrochemical and electrophoretic study of sodium metamizole. *J. Chil. Chem. Soc.*, **2008**, *53*, 1572-1575.

[21] Merkoçi, A.; Pumera, M.; Llopis, X.; Pérez, B.; del Valle, M.; Alegret, S. New materials for electrochemical sensing VI: Carbon nanotubes. *Trends Anal. Chem.*, **2005**, *24*, 826-838.

[22] Valentini, F.; Amine, A.; Orlanducci, S.; Terranova, M.L.; Palleschi, G. Carbon nanotube purification: Preparation and characterization of carbon nanotube paste electrodes. *Anal. Chem.*, **2003**, *75*, 5413-5421.

[23] Rivas, G.A.; Rubianes, M.D.; Rodríguez, M.C.; Ferreyra, N.F.; Luque, G.L.; Pedano, M.L.; Miscoria, S.A.; Parrado, C. Carbon nanotubes for electrochemical biosensing. *Talanta*, **2007**, *74*, 291-307.

[24] Agüí, L.; Yáñez-Sedeño, P.; Pingarrón, J.M. Role of carbon nanotubes in electroanalytical chemistry – A review. *Anal. Chim. Acta*, **2008**, *622*, 11-47.

[25] Wildgoose, G.G.; Banks, C.E.; Leventis, H.C.; Compton, R.G. Chemically modified carbon nanotubes for use in electroanalysis. *Microchim. Acta*, **2006**, *152*, 187-214.

[26] Banks, C.E.; Compton, R.G. Exploring the electrocatalytic sites of carbon nanotubes for NADH detection: an edge plane pyrolitic graphite electrode study. *Analyst*, **2005** *130*, 1232-1239.

[27] Banks, C.E.; Compton, R.G. New electrodes for old: from carbon nanotubes to edge plane pyrolitic graphite. *Analyst*, **2006**, *131*, 15-21.

[28] Gouveia-Caridade, C.; Pauliukaite, R.; Brett, C.M.A. Development of electrochemical oxidase biosensors based on carbon nanotube-modified carbon film electrodes for glucose and ethanol. *Electrochim. Acta*, **2008**, *53*, 6732-6739.

[29] Wang, J.X.; Li, M.X.; Shi, Z.J.; Li, N.Q.; Gu, Z.N. Direct electrochemistry of cytochrome c at a glassy carbon electrode modified with single-wall carbon nanotubes. *Anal. Chem.*, **2002**, *74*, 1993-1997.

[30] Zhao, G.C.; Yin, Z.Z.; Zhang, L.; Wei, X.W. Direct electrochemistry of cytochrome c on a multi-walled carbon nanotubes modified electrode and its electroanalytic activity for the reduction of H_2O_2. *Electrochem. Commun.*, **2005**, *7*, 256-260.

[31] Yin, Y.J.; Wu, P.; Lu, Y.F.; Du, P.; Shi, Y.M.; Cai, C.X. Immobilization and direct electrochemistry of cytochrome C at a single-walled carbon nanotube-modified electrode. *J. Solid State Electrochem.*, **2007**, *11*, 390-397.

[32] Zhao, Q.; Gan, Z.H.; Khuang, Q.K. Electrochemical sensors based on carbon nanotubes. *Electroanalysis*, **2002**, *14*, 1609-1613.

[33] Saini, R.K.; Chiang, I.W.; Peng, H.Q.; Smalley, R.E.; Billups, W.E.; Hauge, R.H.; Margrave, J.L. Covalent sidewall functionalization of single wall carbon nanotubes. *J. Am. Chem. Soc.*, **2003**, *125*, 3617-3621.

[34] Chen, J.; Hamon, M.A.; Hu, H.; Chen, Y.; Rao, A.M.; Eklund, P.C.; Haadon, R.C. Solution properties of single walled carbon nanotubes. *Science*, **1998**, *282*, 95-98.

[35] Islan, M.F.; Rojas, E.; Bergey, D.M.; Johson, A.T.; Yodh, A.G. High weight fraction surfactant solubilization of single-wall carbon nanotubes in water. *Nano Lett.*, **2003**, *3*, 269-273.

[36] Star, A.; Stoddart, J.F.; Steuerman, D.; Diehl, M.; Boukai, A.; Wong, E.W.; Yang, X.; Chung, S.W.; Choi, H.; Heath, J.R. Preparation and properties of polymer-wrapped single-walled carbon nanotubes. *Angew. Chem. Int. Ed.*, **2001**, *40*, 1721-1725.

[37] Yi, H.; Wu, L.Q.; Bentley, W.E.; Ghodss, R.; Rubloff, G.W.; Culver, J.N.; Payne, G.F. Biofabrication with chitosan. *Biomacromolecules*, **2005**, *6*, 2881-2894.

[38] de Oliveira, I.R.W.Z.; Vieira, I.C. Immobilization procedures for the development of a biosensor for determination of hydroquinone using chitosan and gilo (Solanum gilo). *Enzyme Microbial. Technol.*, **2006**, *38*, 449-456.

[39] Wan, Y.; Creber, K.A.M.; Peppley, B.; Bui, V.T. Ionic conductivity of chitosan membranes. *Polymer*, **2003**, *44*, 1057-1065.

[40] Deng, Y.; Liu, D.; Du, G.; Li, X.: Chen, J. Preparation and characterization of hyaluronan /chitosan scaffold cross-linked by 1-ethyl-3-(3-dimethylaminopropyl) carbodiimide. *Polymer Internat.*, **2007**, *56*, 738-745.

[41] Cruz, J.; Kawasaki, M.; Gorski, W. Electrode coatings based on chitosan scaffolds. *Anal. Chem.*, **2000**, *72*, 680-686.

[42] Fagury, R.L.R.P.; Lupetti, K.O.; Fatibello-Filho, O. Flexible potentiometric minisensor based on manganese dioxide-composite for the determination of hydrogen peroxide in bleach and pharmaceutical products. *Anal. Lett.*, **2005**, *38*, 1857-1867.

[43] Pauliukaite, R.; Ghica, M.E.; Fatibello-Filho, O.; Brett, C.M.A. Comparative study of different cross-linking agents for the immobilization of functionalized carbon nanotubes within a chitosan film supported on a graphite-epoxy composite electrode. *Anal. Chem.*, **2009**, *81*, 5364-5372.

[44] Ghica, M.E.; Pauliukaite, R.; Fatibello-Filho, O.; Brett, C.M.A. Application of functionalised carbon nanotubes immobilised into chitosan films in amperometric enzyme biosensors. *Sens. Actuat. B*, **2009**, *142*, 308-315.

[45] Muralidharan, B.; Gopu, G.; Vedhi, C.; Manisankar, P. Determination of analgesics in pharmaceutical formulations and urine samples using nano polypyrrole modified glassy carbon electrode. *J. Appl. Electrochem.*, **2009**, *39*, 1177-1184.

[46] Wessel, J.C.; Matyja, M.; Neugebauer, M.; Kiefer, H.; Daldrup, T.; Tarbah, F.A., Weber, H. Characterization of oxalic acid derivatives as new metabolites of metamizol (dipyrone) in incubated hen´s egg and human. *Eur. J. Pharm. Sci.*, **2006**, *28*, 15-25.

[47] Pauliukaite, R.; Ghica, M.E.; Fatibello-Filho, O.; Brett, C.M.A. Electrochemical impedance studies of chitosan-modified electrodes for application in electrochemical sensors and biosensors. *Electrochim. Acta*, **2010**, in press.

[48] Marcolino-Júnior, L.H.; Bergamini, M.F.; Teixeira, M.F.S.; Cavalheiro, E.T.G.; Fatibello-Filho, O. Flow injection amperometric determination of dipyrone in pharmaceutical formulations using a carbon paste electrode. *Il Farmaco*, **2003**, *58*, 999-1004.

Received: November 11, 2009 **Revised: December 17, 2009** **Accepted: December 19, 2009**